processes

MDPI

Article

Thermodynamic Optimization of a Geothermal Power Plant with a Genetic Algorithm in Two Stages

Mehdi A. Ehyaei [1,*], Abolfazl Ahmadi [2], Marc A. Rosen [3] and Afshin Davarpanah [4,*]

1 Department of Mechanical Engineering, Pardis Branch, Islamic Azad University, Pardis New City 1468995513, Iran
2 Department of Energy Systems, School of New Technologies, Iran University of Science and Technology, Tehran 1584743311, Iran; a_ahmadi@iust.ac.ir
3 Faculty of Engineering and Applied Science, University of Ontario Institute of Technology, 2000 Simcoe Street North, Oshawa, ON L1G 0C5, Canada; marc.rosen@uoit.ca
4 Department of Mathematics, Aberystwyth University, Aberystwyth SY23 3FL, UK
* Correspondence: aliehyaei@pardisiau.ac.ir (M.A.E.); afd6@aber.ac.uk (A.D.)

Received: 29 August 2020; Accepted: 9 October 2020; Published: 12 October 2020

Abstract: Due to the harmful effects and depletion of non-renewable energy resources, the major concerns are focused on using renewable energy resources. Among them, the geothermal energy has a high potential in volcano regions such as the Middle East. The optimization of an organic Rankine cycle with a geothermal heat source is investigated based on a genetic algorithm having two stages. In the first stage, the optimal variables are the depth of the well and the extraction flow rate of the geothermal fluid mass. The optimal value of the depth of the well, extraction mass flow rate, and the geothermal fluid temperature is found to be 2100 m, 15 kg/s, and 150 °C. In the second stage, the efficiency and output power of the power plant are optimized. To achieve maximum output power as well as cycle efficiency, the optimization variable is the maximum organic fluid pressure in the high-temperature heat exchanger. The optimum values of energy efficiency and cycle power production are equal to 0.433 MW and 14.1%, respectively.

Keywords: geothermal cycle; organic Rankine cycle; optimization; genetic algorithm

1. Introduction

Geothermal energy is heat from the inner part of the earth that is present in rocks and water in cracks and pores within the rock of the earth's crust. The temperature normally increases with depth, although not in a constant manner [1–4]. The benefits of geothermal energy include reduced pollution and avoidance of change in ecosystems' reliability and renewability. It can also provide development opportunities for remote areas. The disadvantages include causing instability in earth structures due to extensive use and corrosion caused by sulfur compounds in geothermal fluids [5–8].

Much research has been carried out on geothermal energy. Drozdz [9] analyzed methods of optimizing geothermal energy conversion. The optimization of the behavior of different types of geothermal energy sources, accounting for constant and dynamic parameters, was presented.

The results show that the variation of unit heat and electrical energy costs affects the optimal pumping intensity.

Jalilinasrabady et al. [10] optimized a single-circuit cycle of the Sabalan geothermal power plant, which is currently under development in northwestern Iran, with exergy methods. To obtain efficient optimal energy, a two-circuit cycle was also examined for power generation. Under these conditions, if the cycle higher pressure, lower pressure, and condenser pressure are 7.5, 1.1, and 0.1 bar respectively, the plant's energy efficiency can reach 49.7%.

Salah and Dincer [11] analyzed the thermodynamics, economics, and optimization of an organic Rankine cycle (ORC) using geothermal sources based on energy and exergy. The results showed that the heat exchanger and condenser have the highest amount of exergy loss, accounting for about 75% of the total exergy loss of the system. Similar research was done by Imran et al. [12] and Yang and Yeh [13].

Heberle et al. [2] studied an ORC with geothermal sources. A combination of heat and power generation for the geothermal sources was proposed at a temperature below 450 K. The results showed that the best choice of working fluid is R227a.

Nami et al. [14] assessed a two-stage ORC with a geothermal source using conventional and advanced exergy analyses. The exergy loss in each component was divided into internal, external, avoidable, and unavoidable exergy losses parts. Advanced exergy analysis showed that only 15% of the exergy loss in the condenser is avoidable. The condenser exergy loss is about 7% of the cycle exergy losses.

Astolfi et al. [15] optimized an ORC techno-economically for an off-design state. They showed that the electrical production of the system could be increased by using a novel system to release condenser heat. Similar research was done for transient conditions [16].

Liu et al. [17] investigated several configurations and working fluids of ORC cycles, to help designers select the optimum case for different operation conditions. Behzadi et al. [18] examined the optimization of a system including an absorption chiller, an ORC, and photovoltaic with geothermal energy sources. They used a multi-objective genetic algorithm for optimization. With optimization, the exergy efficiency of the system reached 12.3%.

Several studies have been reported in recent years on energy, exergy, economic and environmental analyses, and optimization of various power generation systems, including combined heat and power, renewable energy, and other plants [19–27].

The literature suggests that the optimization of an ORC cycle using a geothermal energy source, taking into account the effects of the geothermal well depth and mass flow rate of the geothermal fluid, has not been done yet. The aim of this paper, therefore, is to optimize an organic Rankine cycle with a geothermal heat source based on energy-exergy methods. After energy and exergy modeling of the cycle of the geothermal power plant, an optimization phase is implemented using a genetic algorithm, in which the depth of the well is calculated as the depth at which the construction of the power plant is economically feasible.

2. Mathematical Modeling

Figure 1 presents a schematic diagram of an organic Rankine cycle (ORC) with a geothermal heat source and the related temperature-entropy diagram [28]. The geothermal energy resource of the Damavand region is considered in this article.

According to Figure 1, the output saturated dry steam of the evaporator is directed to the turbine (point 1) and, in a constant temperature and pressure process, the dry saturated steam is expanded in the turbine (point 2) and generates power using a generator. This action reduces the steam pressure and temperature and can involve condensation. The exhaust wet steam from the turbine enters the regenerative system, where the temperature and pressure are reduced (point 3). The output wet saturated steam from the regenerator enters the condenser and is converted to a saturated fluid (point 4). The ORC working fluid is cooled by cooling water supplied from the cooling tower. By converting the saturated steam to liquid in a condenser, a turbine and a vacuum condenser are created, and the pressure drop behind the turbine increases the power plant efficiency and power output. The saturated liquid from the condenser is pumped to a higher pressure (points 4 and 5), and the output saturation fluid from the high-pressure pump enters the regenerator and is heated (point 6). The output high-pressure saturated fluid from the heat regenerator enters into a heat exchanger and is heated to a dry saturated vapor in a constant pressure process by the geothermal heat source. The dry saturated steam enters the turbine.

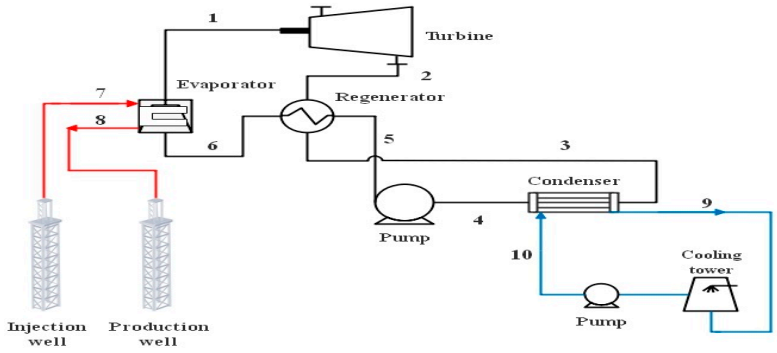

(**a**)

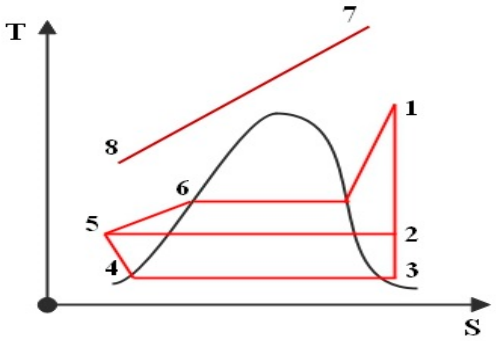

(**b**)

Figure 1. (**a**) Organic Rankine cycle (ORC) with the geothermal heat source, (**b**) the associated temperature-entropy diagram.

The main assumptions used in this study are as follows [18,29,30]:

(1) The process is a steady-state and continuous flow type.
(2) The processes in the turbine and the pump are polytropic.
(3) The evaporative and condensing efficiencies are both 80%.
(4) The isentropic efficiencies of the turbine and pump are both 80%.

A general equation for mass conservation is as follows [31]:

$$\left(\frac{dm_{C.V.}}{dti}\right) = \sum_{out} \dot{m} - \sum_{in} \dot{m} = 0 \quad (1)$$

where $\dot{m}$ is the mass flow rate (kg/s) and the subscripts in and out denote input and output.

A general equation for energy conservation is as follows [31]:

$$\dot{Q}_{C.V.} + \dot{W}_{C.V.} + \sum_{in}\left(h + \frac{V^2}{2} + gZ\right)\dot{m} \pm \sum_{out}\left(h + \frac{V^2}{2} + gZ\right)\dot{m} = \left(\frac{dE_{C.V.}}{dti}\right) \quad (2)$$

where $\dot{Q}_{C.V.}$ is input heat rate (kW), $\dot{W}_{C.V.}$ is work production rate (kW), h is specific enthalpy (kJ/kg), $\frac{V^2}{2}$ represents specific kinetic energy (m/s), gZ represents potential energy (m^2/s^2), $\dot{m}$ is mass flow rate (kg/s), and $\left(\frac{dE_{C.V.}}{dt}\right)$ is a time-dependent term denoting the energy storage rate in the control volume. For steady-state conditions, the last term becomes zero.

Mass and energy conservation equations for the various components in the cycle are given in Table 1. In this table, $\dot{W}$ and n are respectively the power produced (kW) and the energy efficiency, $\dot{m}$ is

the mass flow rate (kg/s), h is the specific enthalpy (kJ/kg), $\dot{Q}$ is the rate of heat transfer (kW), and ε_{rec} is the effectiveness of the regenerator.

Table 1. Mass and energy conservation equations for various components of the cycle.

Component	Mass Conservation	Energy Conservation
Pump	$\dot{m}_4 = \dot{m}_5$	$\dot{W}_{Pump} = \left[\frac{\dot{m}_4}{n_{Pump}}(h_5 - h_4)\right]$
Turbine	$\dot{m}_1 = \dot{m}_2$	$\dot{W}_{Turbine} = \dot{m}_1 \times n_{Turbine}(h_1 - h_2)$
Evaporator	$\dot{m}_6 = \dot{m}_1$ $\dot{m}_7 = \dot{m}_8$	$\dot{Q}_{Evaporator} = \dot{m}_6(h_1 - h_6)$ $\dot{Q}_{Geothermal.in} = \dot{m}_7(h_7 - h_8)$
Condenser	$\dot{m}_3 = \dot{m}_4$ $\dot{m}_{10} = \dot{m}_9$	$\dot{Q}_{Condenser} = \dot{m}_3(h_3 - h_4)$
Regenerator	$\dot{m}_2 = \dot{m}_3$ $\dot{m}_5 = \dot{m}_6$	$\varepsilon_{reg} = \left(\frac{h_2 - h_3}{q_{Reg,max}}\right) = \left(\frac{h_2 - h_3}{h_2 - h_{3,min}}\right)$

The cycle energy efficiency and the specific work output respectively can be written as follows [31]:

$$n_{en} = \left[\frac{\left(\dot{W}_{Turbine} - W_{Pump}\right)}{\dot{Q}_{Geothermal.in}}\right] \tag{3}$$

$$w = \left[\frac{\left(\dot{W}_{Turbine} - W_{Pump}\right)}{\dot{m}}\right] \tag{4}$$

Exergy analysis, which is based on the second law of thermodynamics, allows the irreversibility of a system to be considered and calculated. The exergy loss rate for a system at the steady-state process can be written as follows [31]:

$$\dot{E}x_d = \dot{E}x_Q - \dot{E}x_W + \sum_{in} \dot{m}e - \sum_{out} \dot{m}e \tag{5}$$

where $\dot{E}x_d$ is the exergy loss rate (kW), $\dot{E}x_Q$ and $\dot{E}x_W$ are the exergy rates associated with the heat rate and work rate respectively, of the control volume (kW), $\dot{m}$ is the mass flow rate (kg/s), and e is specific exergy (kJ/kg).

The exergy rates associated with heat and power, and the exergy destruction rate, can be expressed respectively as follows [31]:

$$\dot{E}x_Q = \sum\left(1 - \frac{T}{T_{env}}\right)\dot{Q} \tag{6}$$

$$\dot{E}x_W = \dot{W}_{net} \tag{7}$$

$$\dot{E}x_d = \sum\left(1 - \frac{T}{T_0}\right)\dot{Q}_{net} - \dot{W}_{net} + \sum_{in} \dot{m}e - \sum_{out} \dot{m}e \tag{8}$$

Here, the subscript env denotes the state of the environment, and T and T_{env} respectively, are the temperature and reference environment temperature (K).

The exergy flow rate and the specific exergy of mass flow can be written respectively as [31]:

$$\dot{E} = \dot{m}e \tag{9}$$

$$e = [h - h_e - T_{env}(s - s_0)] \tag{10}$$

where, s and s_0 are the specific entropy and specific entropy at the reference environment state (kJ/kg·K), $\dot{E}$ is the exergy flow rate (kW), e is specific exergy (kJ/kg), and h and h_0 respectively are specific enthalpy and specific enthalpy at the reference environment state (kJ/kg).

The exergy loss rate in the form of exergy destruction is dependent on the total entropy generation rate of each of the system components, and can be written as follows [31]:

$$\dot{E}x_d = T_{env} \times \dot{S}_{gen} \tag{11}$$

Expressions for the exergy destruction rate for each system component are given in Table 2.

Table 2. Exergy destruction rate expressions for system components.

Component	Exergy Destruction Rate (kW)
Pump	$\dot{m}_4(e_5 - e_4) - \dot{W}_{Pump}$
Turbine	$\dot{m}_1(e_2 - e_1) - \dot{W}_{Turbine}$
Evaporator	$\dot{m}_6(e_1 - e_6) + \left[\left(1 - \frac{T_0}{T_{Eva}}\right)\dot{Q}_{Evaporator}\right]$
Condenser	$\dot{m}_3(e_4 - e_3) + \left[\left(1 - \frac{T_0}{T_{Cond}}\right)\dot{Q}_{Condenser}\right]$
Regenerator	$\dot{m}_2(e_5 + e_2 - e_6 - e_3)$

The total exergy destruction loss rate equation for the overall system can be expressed as follows [31]:

$$\sum \dot{E}x_{d,total} = \dot{E}x_{d,Pump} + \dot{E}x_{d,Turbine} + \dot{E}x_{d,Cond} + \dot{E}x_{d,Eva} + \dot{E}x_{d,Reg} \tag{12}$$

The cycle exergy efficiency can be expressed as follows [31]:

$$n_{ex} = \left[\frac{\left(\dot{W}_{Turbine} - \dot{W}_{Pump}\right)}{\dot{Q}_{geothermal}\left(1 - \frac{T_0}{T_{geothermal}}\right)}\right] \tag{13}$$

In the geothermal system considered, the outlet geothermal fluid temperature is the main variable that influences the performance of the system. By increasing the geothermal fluid temperature, the thermal efficiency of the power plant increases. As the geothermal fluid temperature increases to 63 °C, the plant's thermal efficiency increases by 5.9%. Based on these data, the relationship between the geothermal fluid temperature and the thermal (energy) efficiency of the power plant can be approximated as follows [32]:

$$n_{th} = 0.0935T_{geothermal} - 2.3266 \tag{14}$$

where, n_{th} is the thermal efficiency of the power plant (%), and T is the geothermal fluid temperature (°C).

The geothermal fluid temperature is dependent on the geothermal well depth as follows [33]:

$$T = 83.92\ln(Z) - 361.16 \tag{15}$$

where Z is the depth of well (m). With this relation, the effect of the geothermal well depth on the geothermal fluid temperature can be described in modeling the geothermal system. The fluid temperature also influences the output power of the system. The geothermal well depth is affected by many restrictions, such as the state of available technology and costs.

A flow chart of the procedure used in the mathematical modeling of the cycle is shown in Figure 2.

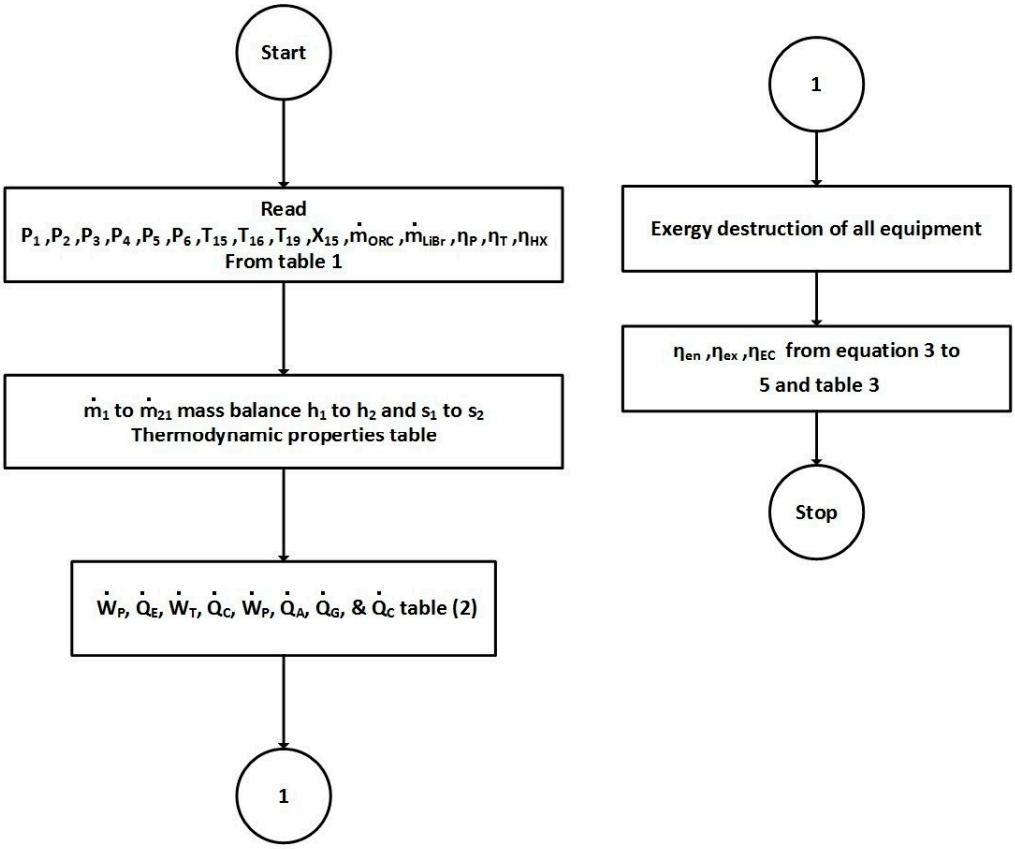

Figure 2. Flow chart of mathematical modeling of the cycle.

3. Genetic Algorithm

The genetic algorithm (GA) is one of the most important metaheuristic algorithms used for optimization for defined functions in a limited domain. In this algorithm, according to the inheritance of the algorithm, past information is extracted and used in the search process. The concepts of the genetic algorithm were developed by Goldberg in 1989. The simulation method discussed below is called an Evolutional Guideline. The Evolutional Guideline simulation method is a kind of neighborhood search method, which functions like a gene [34].

The reasons for selecting the GA are as follows [34]:

- The nature of algorithm random searching in the problem space is somehow considered as a parallel search. Since each of the random chromosomes generated by the algorithm is considered as a new starting point for searching for a part of the state of the problem, the search is performed in all of the chromosomes simultaneously.
- Due to the breadth and dispersion of the points that are being searched, the genetic algorithm yields a good result for objectives that have a great search space.
- The genetic algorithm is considered as a kind of random search and is targeted, and it leads to different results and answers using different approaches.
- The genetic algorithm may have no limit in line with searching and selection of random answers.
- Because of the competition (struggle for existence), the answers and the best choices from the population with high probability will reach the total optimal level.
- The genetic algorithm implementation is simple and requires no complex problem-solving procedures.
- The optimization process can be performed for continuous and discrete variables.
- There is no need to calculate derivative functions.
- Complex cost functions can be optimized with this approach.

- The algorithm is not trapped in local extremes.
- The genetic algorithm can encode variables and perform optimization with encoded variables.
- Encoding speeds up the convergence rate of the algorithm.
- Genetic algorithms use probabilistic transfer rules instead of definite transition rules, meaning that its movement at any point in the algorithm is possible.
- In addition to analytical functions, the algorithm can work with generated numerical data and empirical data.
- The genetic algorithm is capable of optimizing problems with a large number of variables.

Therefore, the genetic algorithm is chosen in this research for the implementation of the optimization problem. A flow chart of the genetic algorithm optimization is shown in Figure 3 [35]. After selection the initial population and lower and upper limits of variables, in the defined domain, the optimum variables are selected.

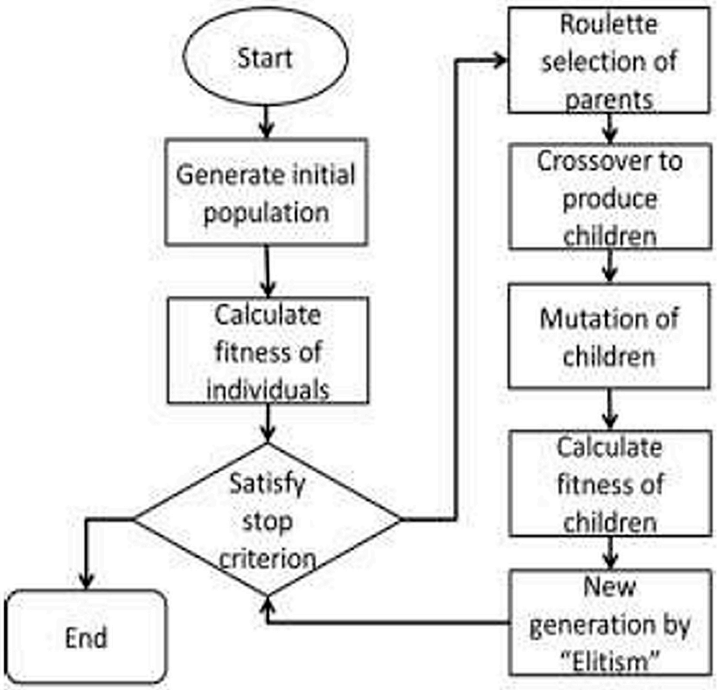

Figure 3. Flow chart of genetic algorithm (GA) optimization [35].

4. Results and Discussion

For the mathematical modeling of the cycle, one code is written in MATLAB software [36]. Refprob software [37] is used for the calculation of thermodynamic properties.

The analysis reported in this paper is based on the geothermal conditions of the city of Damavand, Iran. Damavand, with a longitude 35.7013° N and latitude 52.0586° E, is located near Tehran [38]. The temperature range of the geothermal fluid is about 120 to 170 °C, based on the geothermal production well. The range of pressure is about 3 to 8 bar [39,40].

The organic working fluid used for this cycle is R245fa, a non-flammable, organic fluid. This fluid has a low specific heat and specific volume and has thermodynamic properties suitable for energy recovery. R245fa is from a dry fluid family with good environmental properties, including zero ozone depletion potential and low heat capacity according to the Kigali Amendment to the Montreal Protocol [41].

For validation of the results, Reference [1] is considered. All of the input data and assumptions presented in that article are inserted into the computer program prepared for this article. Table 5 in

Reference [1] that presented the cycle energy and exergy efficiencies is considered for comparison. Figure 4 shows a comparison between the results from mathematical modeling and Reference [1].

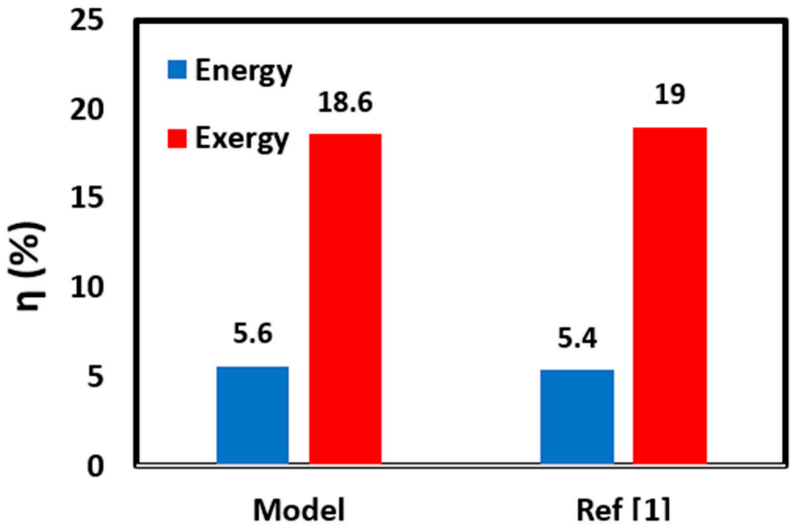

Figure 4. Comparison of efficiencies between mathematical modeling and Reference [1].

Table 3 lists the thermodynamic properties of the working fluid [41]. Table 4 provides the cycle parameter specifications. Table 5 gives the mass flow rates of the different fluids of the cycle. Table 6 lists the results for the Rankine cycle with the geothermal source.

Table 3. Thermodynamic properties of R245fa.

Density (kg/m^3)	Boiling Temperature (°C)	ODP (Ozone Depletion Potential) [−]	T_{bp} (°C)	P_{cr} (MPa)	T_{cr} (°C)	Molar Mass (kg/kmol)
1404.1	15.3	0	14.86	3.639	154.01	134.05

Table 4. Cycle parameter specifications.

Cycle Parameters	Value
P_3	204.6 kPa
P_4	204.6 kPa
P_2	219.82 kPa
P_5	219.82 kPa
P_6	871.18 kPa
P_1	871.18 kPa
T_1	109.9 °C
T_{geo}	150 °C
$T_{cooling}$	20 °C
$\dot{m}_{R245fa}$	12 kg/s
η_{Pump}	0.85
$\eta_{Turbine}$	0.85
$\eta_{Eva,}$	0.80
$\eta_{Condenser}$	0.80
η_{RG}	0.85

Table 5. Mass flow rates for several working fluids in the cycle.

Fluid Mass Flow Rate	Mass Flow Rate (kg/s)
$\dot{m}_{cw}$	6.35
$\dot{m}_{geo}$	15
$\dot{m}_{ORC}$	12

Table 6. Results of thermodynamic analysis of the organic Rankine cycle (ORC) with the geothermal source.

Cycle Parameter	Value
$\dot{Q}_{Eva}$ (kW)	10.8
$\dot{Q}_{Condenser}$ (kW)	8.9
$\dot{W}_{Turbine}$ (kW)	1056.3
$\dot{W}_{Pump}$ (kW)	40.6
$\dot{S}_{gen}$ (kW/K)	121.3
n_{en} (%)	9.3
n_{ex} (%)	11.4
w (kJ/kg)	19.2

Figure 5 shows the amount of entropy produced by various components of the geothermal organic Rankine cycle. The highest entropy production is related to the evaporator and the lowest to the pump.

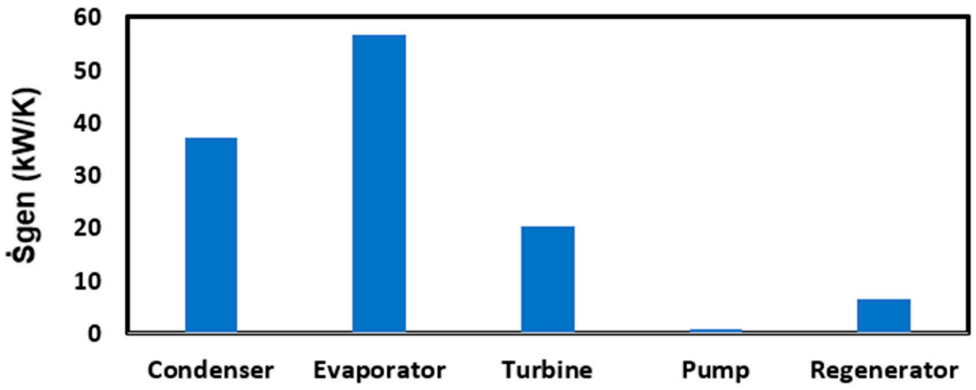

Figure 5. Entropy generation rate of cycle components.

The optimization process in this paper occurs in two stages. In the first stage, the optimal geothermal well depth and mass flow rate of geothermal fluid are calculated based on the maximum energy efficiency and the minimum entropy generation rate. The output from this optimization stage is the optimal working point, including the temperature of the inlet fluid (and well depth) and its flow rate. The results of the first stage of optimization are used in the final stage, where the optimal design of the ORC for the calculated point of the previous stage is determined. In the first stage of optimization, the geothermal power output that can be obtained for a geothermal well depth and fluid mass flow rate that leads to the highest energy efficiency and the lowest amount of entropy production rate is determined. Naturally, the greater the depth of the well, the greater the geothermal fluid temperature and the output power. But, increasing the depth of the well increases the cost. So, there is an optimal well depth, for which suitable power is achieved and the costs are minimal. In this section, the optimization of the ORC with a geothermal source is performed using a genetic

algorithm to increase efficiency and thus reduce geothermal fluid use. Note that the reduction of geothermal fluid consumption in this study means that the 'fuel' of a geothermal power plant is simply the outlet fluid from a geothermal well. The cost of this fuel is mainly the cost of constructing, maintaining, and operating the well, as well as any taxes relating to the utilization of geothermal fluids. The efficiency of the power plant is dependent on the geothermal fluid's temperature. The parameters and their ranges used in the first stage of optimization are as follows:

$$\begin{gathered} 2000\ \text{m} < z < 3000\ \text{m} \\ 10\ \text{kg/s} < \dot{m}_{geo} < 50\ \text{kg/s} \\ \text{Target function}: \ \eta_{en} \text{ and } \dot{W}_{net} \end{gathered} \tag{16}$$

Figure 6 shows the convergence of the genetic algorithm and the process of reducing energy efficiency with the population number. The depth of the well varies between 2000 and 3000 m and the fluid flow rate ranges between 10 and 50 kg/s. The number of the population is selected as 20 and the number of generations as 1000. As can be seen in Figure 6, after about 80 repetitions, the optimal value of the energy efficiency is obtained, and further, population number increases to ensure that the optimal point is not local and but instead is a global optimal point.

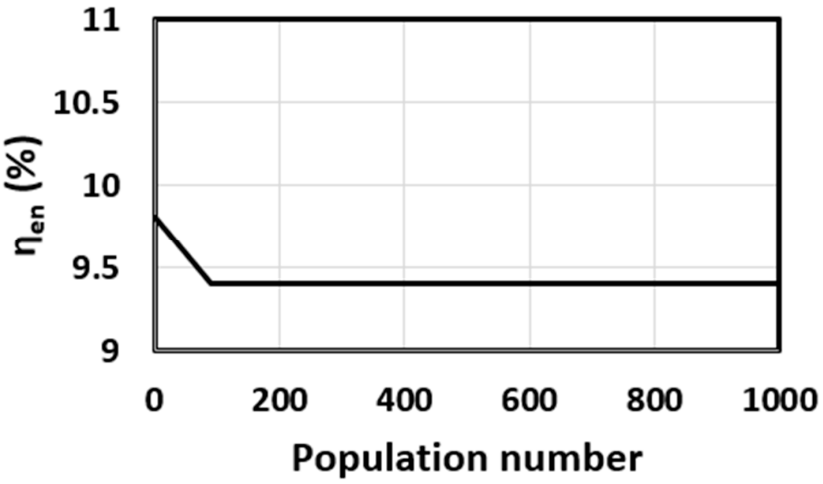

Figure 6. Genetic algorithm convergence and energy efficiency reduction process.

In optimization problems, achieving global optimal points and not optimal local points (if any exist) is important. To do this, there are two general methods:

1- Restarting
2- Changing the initial point

The effect of restarting on the final result for the optimal point is given in Table 7.

Table 7. Effect of restarting on the final results of the genetic algorithm.

Iteration	[pop, G]	[pc, pm]	Optimum Geothermal Well Depth (m)	Optimum Fluid Mass Flow Rate (kg/s)
1	(20, 1000)	(2.7, 0.0)	2101.3	15
2	(20, 1000)	(2.7, 0.0)	2108.7	15.1
3	(20, 1000)	(2.7, 0.0)	2106.5	15.1
4	(20, 1000)	(2.7, 0.0)	2103.4	15
5	(20, 1000)	(2.7, 0.0)	2102.5	15

Table 7 shows that restarting the algorithm does not result in finding multiple optimal points; with every repeat, a point is reported with acceptable accuracy. In Table 7, pop and *G* denote the number of population and generation respectively, while pc and pm denote combination and mutations factors.

Table 8 determines the effect of choosing different initial values on the final optimal result and confirms the lack of dependence of the algorithm on restarting the path and guessing the initial points. The number of considered genes is also analyzed in Table 9, from which it can be concluded that the number of genes has no significant effect on solving and that the solving procedure is almost independent of the number of selected genes in the algorithm.

Table 8. Effect of selecting different start points on the final results of the genetic algorithm.

Initial Value (Depth (m), Mass Flow Rate (kg/s))	[pop, G]	[pc, pm]	Optimum Geothermal Well Depth (m)	Optimum Fluid Mass Flow Rate (kg/s)
(2000, 10)	(20, 1000)	(2.7, 0.0)	2102.7	15.02
(2200, 20)	(20, 1000)	(2.7, 0.0)	2103.3	15.03
(2400, 30)	(20, 1000)	(2.7, 0.0)	2103	15.03
(2600, 40)	(20, 1000)	(2.7, 0.0)	2105.4	15.05
(2800, 50)	(20, 1000)	(2.7, 0.0)	2107.5	15.07

Table 9. Effect of gene number in the genetic algorithm on the final results.

[pop]	[G]	Optimum Depth (m)	Optimum Mass Flow Rate (kg/s)
10	1000	2101.4	15.01
15	1000	2106.5	15.06
20	1000	2102.3	15.02
40	1000	2107.5	15.07
70	1000	2108.4	15.08

The results of the first stage of optimization indicate that:

- The mass flow rate of the geothermal fluid into the cycle is 15 kg/s,
- The depth of the geothermal well is 2100 m and, from Equation (14), the temperature is 150 °C.

The results of the second stage of optimization of the ORC with the geothermal heat source are determined with these inputs. As can be seen from the results of Tables 8 and 9, the cycle energy input is the geothermal fluid and coolant fluid. Geothermal water enters the cycle at a mass flow rate of 15 kg/s and a temperature of 150 °C and leaves the cycle at a temperature of 106.9 °C. The cooling water is introduced into the cycle at a mass flow rate of 6.35 kg/s and a temperature of 20 °C and leaves at a temperature of 43.1 °C. The heat input rate from the geothermal source is 2699.7 kW, of which about 250 kW leaves the cycle as useful power. In the second stage of optimization, the studied variable is the maximum organic fluid pressure in the high-temperature evaporator, and the target function is first selected as the output power of the cycle and then as the thermal efficiency of the cycle. Figure 7 shows that an increase in evaporator pressure to 600 kPa results in an improvement of the cycle power production to 433 kW, which represents the optimum output power for the cycle. By increasing the maximum pressure from the optimum value to the next level, while increasing the power consumption of the pump and decreasing the heat transfer between the geothermal fluid and the working fluid, the total output power of the cycle decreases.

Figure 7 shows the effect of the high-pressure value in the power plant on the cycle output power.

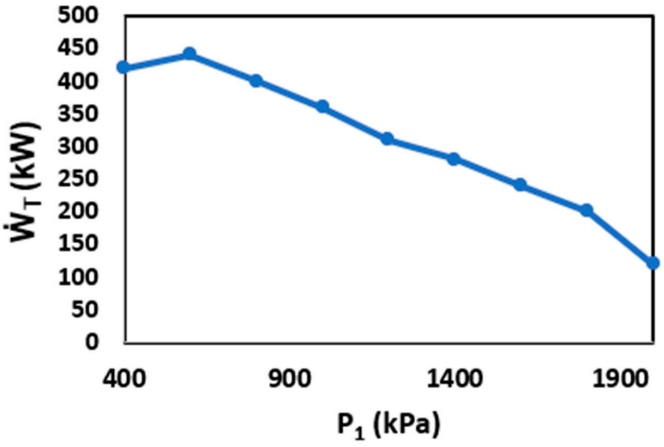

Figure 7. Effect of maximum pressure on cycle output power.

To achieve the best system efficiency, it is necessary to consider the thermal efficiency of the cycle along with the power output of the power plant. Table 10 presents the results of optimizing the ORC with the geothermal heat source. Optimum evaporator pressures for maximum energy efficiency and maximum power production are different.

Table 10. Results of optimization of the organic Rankine cycle with MATLAB.

Target Function	Optimum Evaporator Pressure (MPa)	Value of Target Function at the Specific Optimum Point
n_{en}(%)	2	14.1
$\dot{W}_{net}$ (MW)	6.03	433.06

To better understand the results of this optimization, the change of target functions concerning an independent variable in graphical form is presented. Figure 8 shows the variation of energy efficiency with the evaporator pressure. It is observed in Figure 8 that the effect of increasing the evaporator pressure results in an improvement in the energy efficiency of the cycle. For an evaporator pressure of 2 MPa, the energy efficiency reaches 14.1%. Finally, the effect of varying the evaporator pressure results in:

(1) An improvement in the thermal efficiency of the cycle up to pressure 2 MPa.
(2) An increase in the cycle output power up to a pressure of 0.6 MPa and a reduction in the cycle output power above a pressure 0.6 MPa.

As shown in Figure 8, increasing the higher pressure of the power plant leads to improved energy efficiency, but this does not always mean increasing output power.

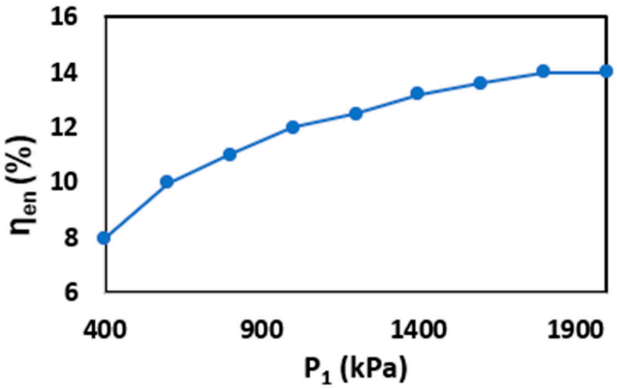

Figure 8. Effect of evaporator pressure on thermal efficiency.

In an ORC driven by fossil fuels, achieving the maximum efficiency means optimal use of the energy source. But, in the geothermal ORC, since geothermal energy is a type of renewable energy, it is necessary to achieve the maximum production capacity to realize the economic objectives of the system. Table 11 lists the values of the main parameters of the cycle before and after optimization.

Table 11. Values of the main parameters of the cycle before and after optimization.

Parameter	Units	Simulation Results	Optimization Results
n_{th}	%	9.3	9.9
n_{ex}	%	11.4	11.9
$\dot{S}_{gen}$	kW/K	121.3	117.3
w	kJ/kg	19.2	20.1

5. Conclusions

An organic Rankine cycle using a geothermal heat source was successfully optimized using energy and exergy analyses. After analyzing the energy and exergy parameters of the geothermal cycle, a two-stage optimization procedure was carried out. In the first stage, the optimal operating point for the power plant was determined. This point is where the cost of the power plant is minimized regarding the optimum mass flow rate and depth of the geothermal well. For the drilling cost of the geothermal well in US$, the equation $16.5z^{1.607}$ [42] (z in meter) is considered. This point is where the cost of the power plant is minimized. The output of this optimization stage leads to an optimal operating point, including the temperature of the inlet fluid (which correlates with the geothermal well depth) and its flow rate. The following results were obtained:

- Optimal values for the depth of the geothermal well, the geothermal extraction mass flow rate, and the geothermal fluid temperature were found to be 2100 m, 15 kg/s, and 150 °C, respectively.
- Values of the energy and exergy efficiencies, the net rate of entropy change, and the specific output power respectively, were determined to be 9.26%, 11.43%, 121.27 kW/K, and 19.21 kJ/kg for the ORC with the geothermal heat source, and 9.87%, 11.88%, 117.27 kW/K, and 20.12 kJ/kg for the optimized ORC with the geothermal heat source.
- Increasing the high pressure of the organic fluid in the evaporator led to an improvement in the thermal efficiency of the cycle. The optimal thermal efficiency for the cycle at a pressure of 2 MPa was found to be 14.1%.

Author Contributions: M.A.E.: Conceptualization, Methodology, Software, Formal analysis, Validation, Visualization, Resources, Writing—Original Draft, Review & Editing, A.A.: Resources, Writing—review & Editing, M.A.R.: Supervision, Writing—review & Editing, A.D.: Writing—review & Editing. All authors have read and agreed to the published version of the manuscript.

Funding: This research received no external funding.

Conflicts of Interest: The authors declare no conflict of interest.

Nomenclature

e	Specific exergy (kJ/kg)
E	Energy (kJ)
$\dot{E}$	Exergy rate (kW)
gZ	Potential energy $\left(m^2/s^2\right)$
G	Number of generation
h	Specific enthalpy $\left(\frac{kJ}{kg}\right)$
m	Mass (kg)

$\dot{m}$	Mass flow rate (kg/s)
pc	Combination factor
pm	Mutation factor
pop	Population number
$\dot{Q}$	Heat transfer rate (kW)
s	Specific entropy (kJ/kgK)
$\dot{S}_{gen}$	Entropy generation rate $\left(kW\ K^{-1}\right)$
T	Temperature (°C, K)
t	Time (s)
V	Velocity (m/s)
$\dot{W}$	Power (kW)
z	Depth of well (m)

Subscripts

bp	Boiling point
cr	Critical
C.V.	Control volume
cw	Cooling water
D	Destruction
geo	Geothermal
o	Reference state
Q	Heat transfer
th	Thermal
W	Work transfer

Greek Symbols

η	Efficiency

Abbreviations

G	Genetic
ODP	Ozone depletion potential
Pop	Population

References

1. Darvish, K.; Ehyaei, M.A.; Atabi, F.; Rosen, M.A. Selection of optimum working fluid for Organic Rankine Cycles by exergy and exergy-economic analyses. *Sustainability* **2015**, *7*, 15362–15383. [CrossRef]
2. Valizadeh, K.; Farahbakhsh, S.; Bateni, A.; Zargarian, A.; Davarpanah, A.; Alizadeh, A.; Zarei, M. A parametric study to simulate the non-Newtonian turbulent flow in spiral tubes. *Energy Sci. Eng.* **2019**. [CrossRef]
3. Hu, X.; Xie, J.; Cai, W.; Wang, R.; Davarpanah, A. Thermodynamic effects of cycling carbon dioxide injectivity in shale reservoirs. *J. Pet Sci. Eng.* **2020**, *195*, 107717. [CrossRef]
4. Shirmohammadi, R.; Aslani, A.; Ghasempour, R.; Romeo, L.M. CO_2 Utilization via Integration of an Industrial Post-Combustion Capture Process with a Urea Plant: Process Modelling and Sensitivity Analysis. *Processes* **2020**, *8*, 1144. [CrossRef]
5. Davarpanah, A.; Mirshekari, B. Experimental Investigation and Mathematical Modeling of Gas Diffusivity by Carbon Dioxide and Methane Kinetic Adsorption. *Ind. Eng. Chem. Res.* **2019**. [CrossRef]
6. Astolfi, M.; Romano, M.C.; Bombarda, P.; Macchi, E. Binary ORC (organic Rankine cycles) power plants for the exploitation of medium–low temperature geothermal sources–Part A: Thermodynamic optimization. *Energy* **2014**, *66*, 423–434. [CrossRef]
7. Saffari, H.; Sadeghi, S.; Khoshzat, M.; Mehregan, P. Thermodynamic analysis and optimization of a geothermal Kalina cycle system using Artificial Bee Colony algorithm. *Renew. Energy* **2016**, *89*, 154–167. [CrossRef]

8. Davarpanah, A.; Zarei, M.; Valizadeh, K.; Mirshekari, B. CFD design and simulation of ethylene dichloride (EDC) thermal cracking reactor. *Energy Sources Part A Recover. Util. Environ. Eff.* **2019**. [CrossRef]
9. Drozdz, M. An optimisation model of geothermal-energy conversion. *Appl. Energy* **2003**, *74*, 75–84. [CrossRef]
10. Jalilinasrabady, S.; Itoi, R.; Valdimarsson, P.; Saevarsdottir, G.; Fujii, H. Flash cycle optimization of Sabalan geothermal power plant employing exergy concept. *Geothermics* **2012**, *43*, 75–82. [CrossRef]
11. El-Emam, R.S.; Dincer, I. Exergy and exergoeconomic analyses and optimization of geothermal organic Rankine cycle. *Appl. Therm. Eng.* **2013**, *59*, 435–444. [CrossRef]
12. Imran, M.; Usman, M.; Park, B.-S.; Kim, H.-J.; Lee, D.-H. Multi-objective optimization of evaporator of organic Rankine cycle (ORC) for low temperature geothermal heat source. *Appl. Therm. Eng.* **2015**, *80*, 1–9. [CrossRef]
13. Yang, M.-H.; Yeh, R.-H. Economic performances optimization of an organic Rankine cycle system with lower global warming potential working fluids in geothermal application. *Renew. Energy* **2016**, *85*, 1201–1213. [CrossRef]
14. Nami, H.; Nemati, A.; Jabbari Fard, F. Conventional and advanced exergy analyses of a geothermal driven dual fluid organic Rankine cycle (ORC). *Appl. Therm. Eng.* **2017**, *122*, 59–70. [CrossRef]
15. Astolfi, M.; La Diega, L.N.; Romano, M.C.; Merlo, U.; Filippini, S.; Macchi, E. Techno-economic optimization of a geothermal ORC with novel "Emeritus" heat rejection units in hot climates. *Renew. Energy* **2019**, *147*, 2810–2821. [CrossRef]
16. Pollet, M.; Gosselin, L.; Dallaire, J.; Mathieu-Potvin, F. Optimization of geothermal power plant design for evolving operating conditions. *Appl. Therm. Eng.* **2018**, *134*, 118–129. [CrossRef]
17. Liu, X.; Wei, M.; Yang, L.; Wang, X. Thermo-economic analysis and optimization selection of ORC system configurations for low temperature binary-cycle geothermal plant. *Appl. Therm. Eng.* **2017**, *125*, 153–164. [CrossRef]
18. Behzadi, A.; Gholamian, E.; Ahmadi, P.; Habibollahzade, A.; Ashjaee, M. Energy, exergy and exergoeconomic (3E) analyses and multi-objective optimization of a solar and geothermal based integrated energy system. *Appl. Therm. Eng.* **2018**, *143*, 1011–1022. [CrossRef]
19. Ebadati, A.; Davarpanah, A.; Shahhoseini, A.; Ahmadi, P. An experimental study to measure the required fresh water and treated water for drilling an unconventional shale reservoir. *Int. J. Environ. Sci. Technol.* **2019**, *16*, 7727–7734. [CrossRef]
20. Aliehyaei, M.; Atabi, F.; Khorshidvand, M.; Rosen, M.A. Exergy, Economic and Environmental Analysis for Simple and Combined Heat and Power IC Engines. *Sustainability* **2015**, *7*, 4411–4424. [CrossRef]
21. Jin, Y.; Davarpanah, A. Using Photo-Fenton and Floatation Techniques for the Sustainable Management of Flow-Back Produced Water Reuse in Shale Reservoirs Exploration. *Water Air Soil Pollut.* **2020**, *231*, 1–8. [CrossRef]
22. Asgari, E.; Ehyaei, M. Exergy analysis and optimisation of a wind turbine using genetic and searching algorithms. *Int. J. Exergy* **2015**, *16*, 293. [CrossRef]
23. Alizadeh, S.M.; Ghazanfari, A.; Ehyaei, M.A.; Ahmadi, A.; Jamali, D.; Nedaei, N.; Davarpanah, A. Investigation the Integration of Heliostat Solar Receiver to Gas and Combined Cycles by Energy, Exergy, and Economic Point of Views. *Appl. Sci.* **2020**, *10*, 5307. [CrossRef]
24. Ghasemian, E.; Ehyaei, M. Evaluation and optimization of organic Rankine cycle (ORC) with algorithms NSGA-II, MOPSO, and MOEA for eight coolant fluids. *Int. J. Energy Environ. Eng.* **2017**, *9*, 39–57. [CrossRef]
25. Kazemi, H.; Ehyaei, M. Energy, exergy, and economic analysis of a geothermal power plant. *Adv. Geo-Energy Res.* **2018**, *2*, 190–209. [CrossRef]
26. Ehyaei, M.; Mozafari, A. Energy, economic and environmental (3E) analysis of a micro gas turbine employed for on-site combined heat and power production. *Energy Build.* **2010**, *42*, 259–264. [CrossRef]
27. Ehyaei, M.; Ahmadi, A.; Assad, M.E.H.; Rosen, M.A. Investigation of an integrated system combining an Organic Rankine Cycle and absorption chiller driven by geothermal energy: Energy, exergy, and economic analyses and optimization. *J. Clean. Prod.* **2020**, *258*, 120780. [CrossRef]
28. Zare, V. A comparative exergoeconomic analysis of different ORC configurations for binary geothermal power plants. *Energy Convers. Manag.* **2015**, *105*, 127–138. [CrossRef]
29. Naseri, A.; Bidi, M.; Ahmadi, M.H. Thermodynamic and exergy analysis of a hydrogen and permeate water production process by a solar-driven transcritical CO_2 power cycle with liquefied natural gas heat sink. *Renew. Energy* **2017**, *113*, 1215–1228. [CrossRef]

30. Naseri, A.; Bidi, M.; Ahmadi, M.H.; Saidur, R. Exergy analysis of a hydrogen and water production process by a solar-driven transcritical CO 2 power cycle with Stirling engine. *J. Clean. Prod.* **2017**, *158*, 165–181. [CrossRef]
31. Bejan, A. *Advanced Engineering Thermodynamics*; John Wiley & Sons: Hoboken, NJ, USA, 2016.
32. Quoilin, S.; Declaye, S.; Tchanche, B.F.; Lemort, V. Thermo-economic optimization of waste heat recovery Organic Rankine Cycles. *Appl. Therm. Eng.* **2011**, *31*, 2885–2893. [CrossRef]
33. Pinti, D.L.; Castro, M.; Shouakar-Stash, O.; Tremblay, A.; Garduño, V.; Hall, C.; Hélie, J.; Ghaleb, B. Evolution of the geothermal fluids at Los Azufres, Mexico, as traced by noble gas isotopes, δ18O, δD, δ13C and 87Sr/86Sr. *J. Volcanol. Geotherm. Res.* **2013**, *249*, 1–11. [CrossRef]
34. Sivanandam, S.; Deepa, S. Genetic Algorithm Optimization Problems. In *Introduction to Genetic Algorithms*; Springer: Berlin/Heidelberg, Germany, 2008; pp. 165–209.
35. Sivaraj, R.; Ravichandran, T. A review of selection methods in genetic algorithm. *Int. J. Eng. Sci. Technol.* **2011**, *3*, 3792–3797.
36. Too, J. Genetic Algorithm for Feature Selection. MATLAB Central File Exchange. Available online: https://www.mathworks.com/matlabcentral/fileexchange/71547-geneticalgorithm-for-feature-selection (accessed on 28 February 2020).
37. Huber, M.; Gallagher, J.; McLinden, M.; Morrison, G. *NIST Standard Reference Database 23, Reference Fluid Thermodynamic and Transport Properties (REFPROP), Version 9.0*; National Institute of Standards and Technology, Thermophysics Division: Boulder, CO, USA, 2020.
38. Farahat, S.; Sarhaddi, F.; Ajam, H. Exergetic optimization of flat plate solar collectors. *Renew. Energy* **2009**, *34*, 1169–1174. [CrossRef]
39. Nazari, Z. The Method of Using Geothermal Energy and Its Potential in Iran. In *International Conference on Management and Energy Planning*; Iranian New Energy Organization: Tehran, Iran, 2012.
40. Nazari, Z. *Geothermal and Solar Energy and its Potential in Iran*; National Iranian Energy Committee: Tehran, Iran, 2013.
41. Guo, T.; Wang, H.; Zhang, S. Fluids and parameters optimization for a novel cogeneration system driven by low-temperature geothermal sources. *Energy* **2011**, *36*, 2639–2649. [CrossRef]
42. Beckers, K.F.; Lukawski, M.Z.; Reber, T.J.; Anderson, B.J.; Moore, M.C.; Tester, J.W. *Tester Introducing Geophires V1.0 Software Package for Estimating Levelized Cost of Eletricity and/or Heat from Enhanced Geothermal Systems*; Stanford University: Stanford, CA, USA, 2013.